Cell Reports, Volume *35*

Supplemental information

DHX15 is required to control RNA virus-induced intestinal inflammation

Junji Xing, Xiaojing Zhou, Mingli Fang, Evan Zhang, Laurie J. Minze, and Zhiqiang Zhang

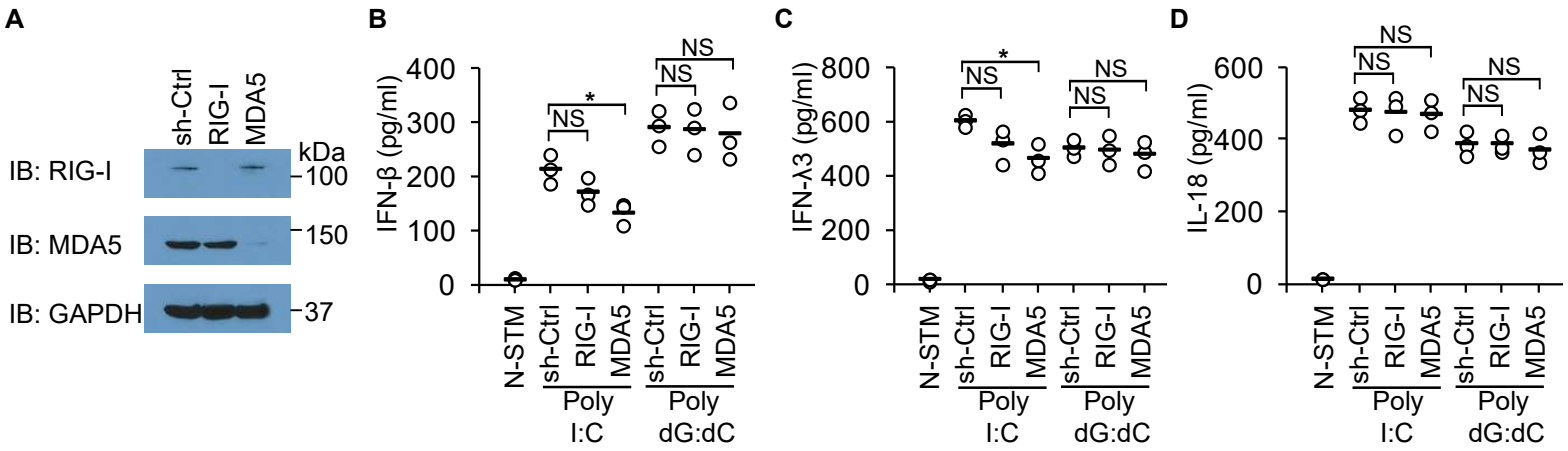

Figure S1. RIG-I and MDA5 play a marginal role in producing IFN-β, IFN-λ3 and IL-18 by human HT-29 IECs after stimulation with poly I:C and poly dG:dC. Related to Figure 1.

(**A**) Immunoblot (IB) showing the knockdown efficiency of shRNAs targeting the indicated genes in HT-29 IECs. Nontargeting shRNA served as a control (sh-Ctrl). GAPDH blots are shown as loading controls. The position of protein markers (shown in kDa) is indicated on the right.

(**B-D**) ELISA of IFN-β (**B**), IFN-λ3 (**C**) and IL-18 (**D**) production from human HT-29 IECs with the indicated shRNA after a 20 h stimulation with 5 μg/ml poly I:C or 2.5 μg/ml poly dG:dC delivered by Lipofectamine 3000. N-STM, scrambled shRNA-treated HT-29 IECs without stimulation. Each circle represents an individual independent experiment and small solid black lines indicate the average of triplicates. NS, $P>0.05$, *$P<0.05$ (unpaired t test).

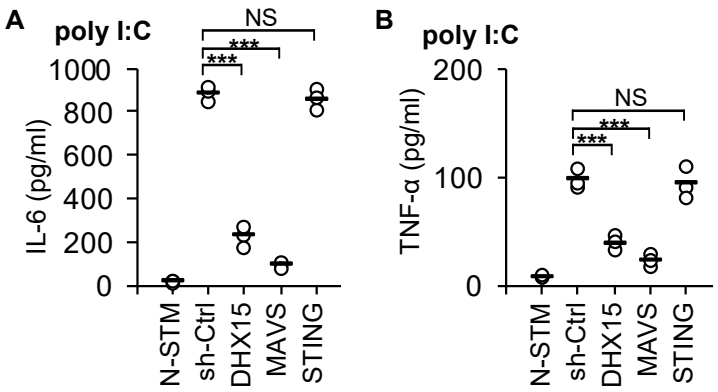

Figure S2. DHX15 positively regulates production of proinflammatory cytokines IL-6 and TNF-α in human HT-29 IECs after poly I:C stimulation. Related to Figure 1.

(**A-B**) ELISA of IL-6 (**A**) and TNF-α (**B**) production from human HT-29 IECs with the indicated shRNA after a 20 h stimulation with 5 μg/ml poly I:C delivered by Lipofectamine 3000. N-STM, scrambled shRNA-treated HT-29 IECs without stimulation. Nontargeting shRNA served as a control (sh-Ctrl). Each circle represents an individual independent experiment and small solid black lines indicate the average of triplicates. NS, $P>0.05$, ***$P<0.001$ (unpaired t test).

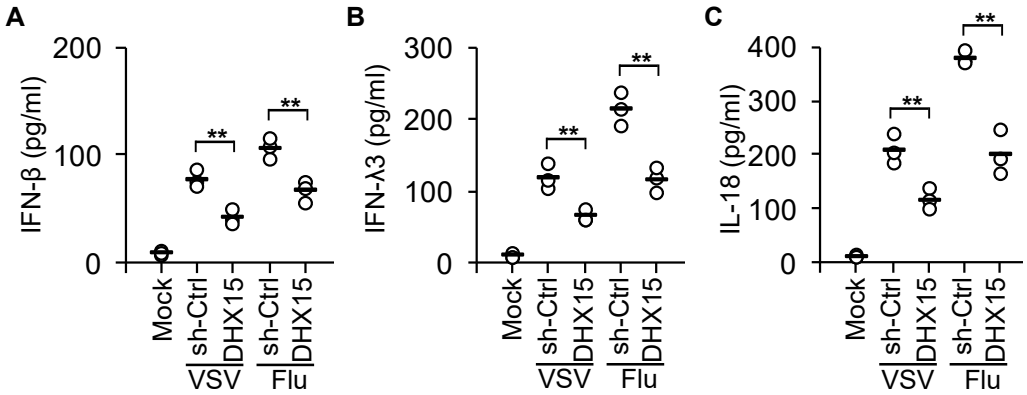

Figure S3. DHX15 is required for IFN-β, IFN-λ3 and IL-18 production in human HT-29 IECs after infection with non-enteric RNA viruses.

Related to Figure 2.

(**A-C**) ELISA of IFN-β (**A**), IFN-λ3 (**B**) and IL-18 (**C**) production from human HT-29 IECs with the indicated shRNA after a 20 h infection with non-enteric RNA viruses including vesicular stomatitis virus Indiana strain (VSV) and influenza A virus PR8 strain (Flu) at a multiplicity of infection (MOI) of 10. Mock, scrambled shRNA(sh-Ctrl)-treated human HT-29 IECs without virus infection. Each circle represents an individual independent experiment and small solid black lines indicate the average of triplicates. **0.001<P<0.01 (unpaired t test).

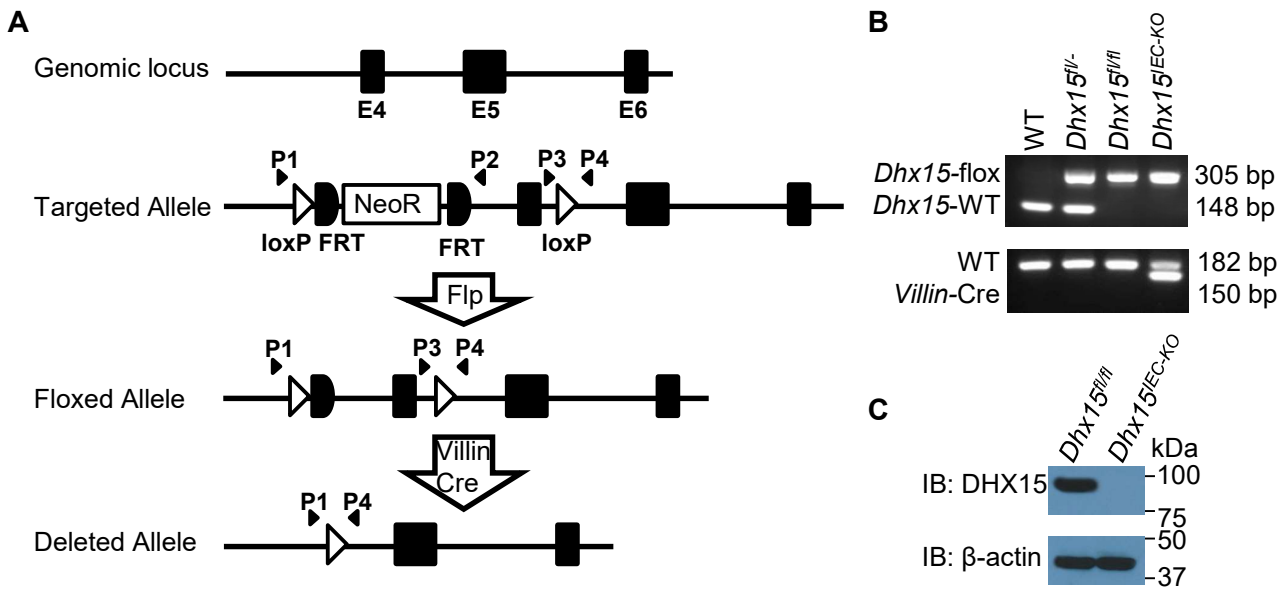

Figure S4. Dhx15 gene targeting. Related to Figure 3.

(**A**) Schematic picture of Dhx15 gene targeting using an FRT-LoxP vector, showing the exons 4 to 6 of Dhx15 gene. Targeted mice were crossed with FRT deleter (Rosa26-FLPe) mice to generate *Dhx15*-floxed (*Dhx15*$^{fl/fl}$) mice, which were further crossed with *Villin*-Cre transgenic mice to generate IEC-specific *Dhx15*-knockout mice, *Dhx15*$^{fl/fl}$; *Villin*-Cre (*Dhx15*$^{IEC\text{-}KO}$).

(**B**) Genotyping PCR to amplify the *Dhx15-flox* (using P1/P2 primer pair) and WT (using P1/P2 primer pair) alleles (top), or the *Villin*-Cre (using 16775/oIMR9074 primer pair) and WT (using 16775/16776 primer pair) alleles (bottom).

(**C**) Immunoblot (IB) of DHX15 in mouse primary IECs from wild-type *Dhx15*$^{fl/fl}$ and *Dhx15*$^{IEC\text{-}KO}$ mice. The position of protein markers (shown in kDa) is indicated on the right.

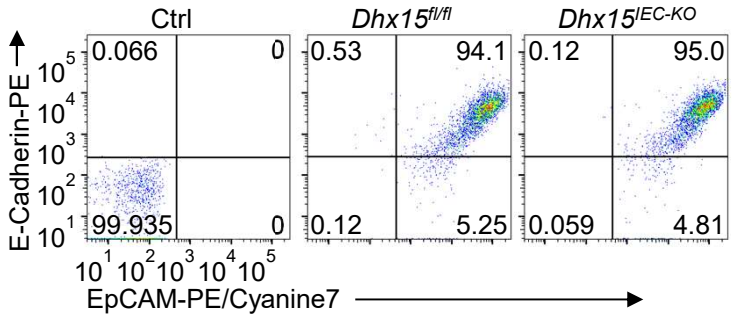

Figure S5. DHX15 does not affect expression of differentiation markers EpCAM and E-Cadherin in mouse IECs. Related to Figure 3.

Flow cytometry analyzing the expression of differentiation markers EpCAM and E-Cadherin in the mouse primary IECs isolated from wild-type *Dhx15*$^{fl/fl}$ and *Dhx15*$^{IEC\text{-}KO}$ mice using isotype control antibodies (Control, Ctrl), EpCAM-PE/Cyanine7 and E-Cadherin-PE antibodies. Flow cytometry data were acquired on a LSR-II flow cytometer (Beckton Dickinson) and analyzed using FlowJo v10 software (Tree Star).

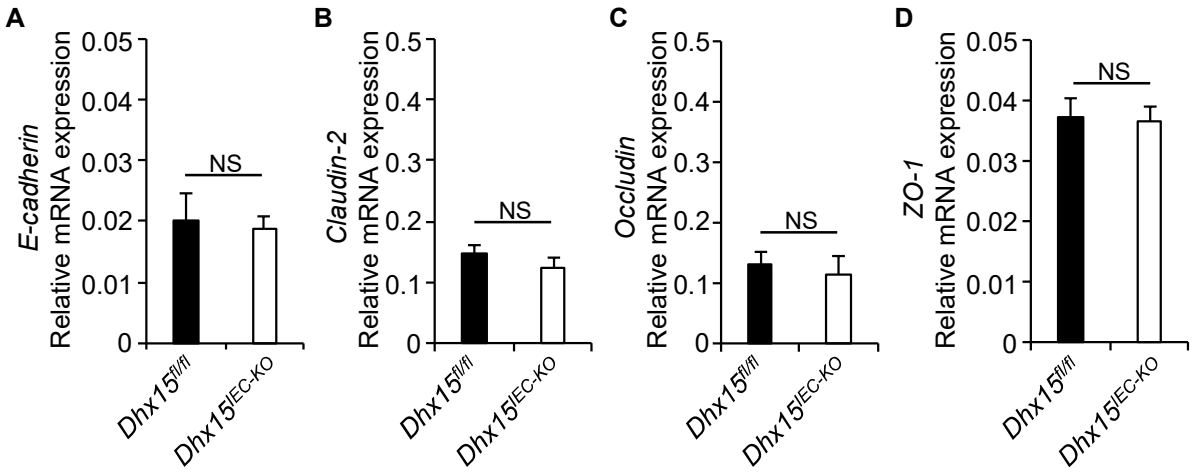

Figure S6. IEC-specific DHX15 ablation does not affect expression of epithelial tight junction proteins. Related to Figure 3.

(**A-D**) The qRT-PCR analysis of the expression of tight junction-related genes E-cadherin (**A**), Claudin-2 (**B**), Occludin (**C**), and Zonula occludens-1 (ZO-1, **D**) in the mouse primary IECs isolated from wild-type *Dhx15*$^{fl/fl}$ and *Dhx15*$^{IEC\text{-}KO}$ mice. mRNA, messenger RNA. NS, not significant.

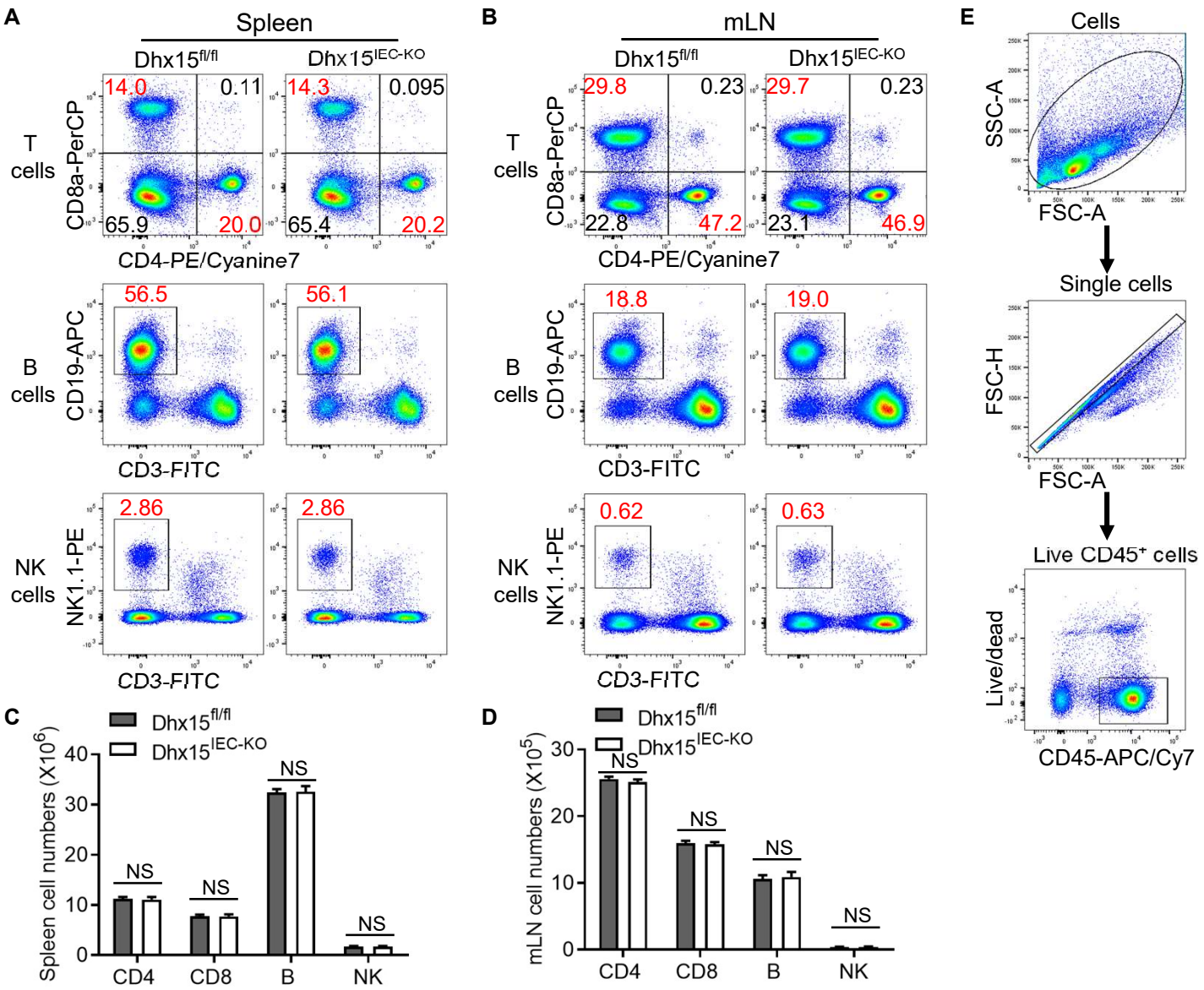

Figure S7. IEC-specific DHX15 deficiency does not affect immune cell subsets frequencies in spleen and mLN. Related to Figure 3.

(**A-B**) Flow cytometry analysis of CD4$^+$ T cells, CD8$^+$ T cells, B cells, and NK cells of spleen cells (**A**) and mesenteric lymph nodes (mLN) (**B**) from wild-type *Dhx15*$^{fl/fl}$ and *Dhx15*$^{IEC\text{-}KO}$ mice using CD3-FITC, CD4-PE/Cyanine7, CD8a-PerCP/Cyanine5.5, CD19-APC and NK1.1-PE antibodies.

(**C-D**) The absolute cell numbers in spleen (**C**) and mLN (**D**) from wild-type *Dhx15*$^{fl/fl}$ and *Dhx15*$^{IEC\text{-}KO}$ mice (n=3 mice) for representative flow cytometry data in **A** and **B**. NS, not significant (unpaired t test).

(**E**) Representative FACS plots showing the gating strategy for analyzing T, B, and NK cell population in spleen of the mice. Flow cytometry data were acquired on a LSR-II flow cytometer (Beckton Dickinson) and analyzed using FlowJo v10 software (Tree Star).

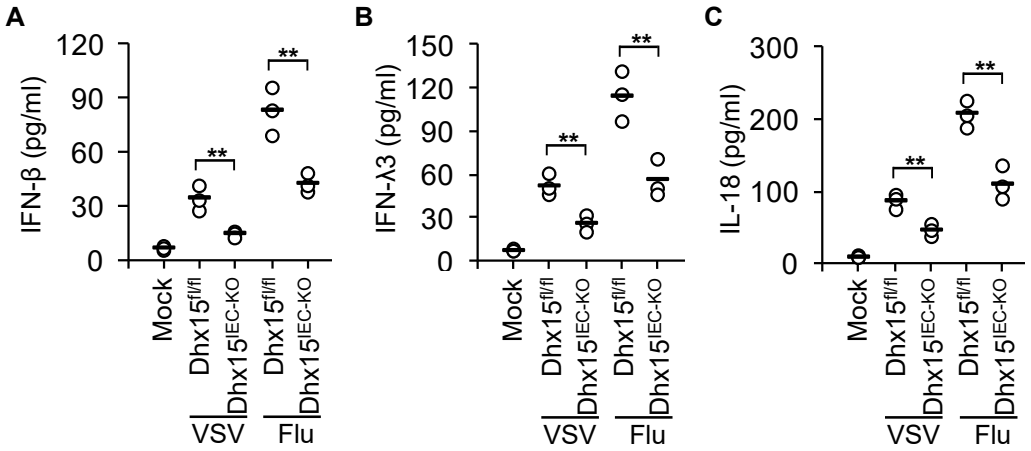

Figure S8. DHX15 positively regulates production of IFN-β, IFN-λ3 and IL-18 in mouse primary IECs after infection with non-enteric RNA viruses. Related to Figure 3.

(**A-C**) ELISA of IFN-β (**A**), IFN-λ3 (**B**) and IL-18 (**C**) production in mouse primary IECs from wild-type *Dhx15*$^{fl/fl}$ and *Dhx15*$^{IEC\text{-}KO}$ mice after a 20 h infection with non-enteric RNA viruses including vesicular stomatitis virus Indiana strain (VSV) and influenza A virus PR8 strain (Flu) at a multiplicity of infection (MOI) of 10. Mock, cells without virus infection. Each circle represents an individual independent experiment and small solid black lines indicate the average of triplicates. **0.001<P<0.01 (unpaired t test).

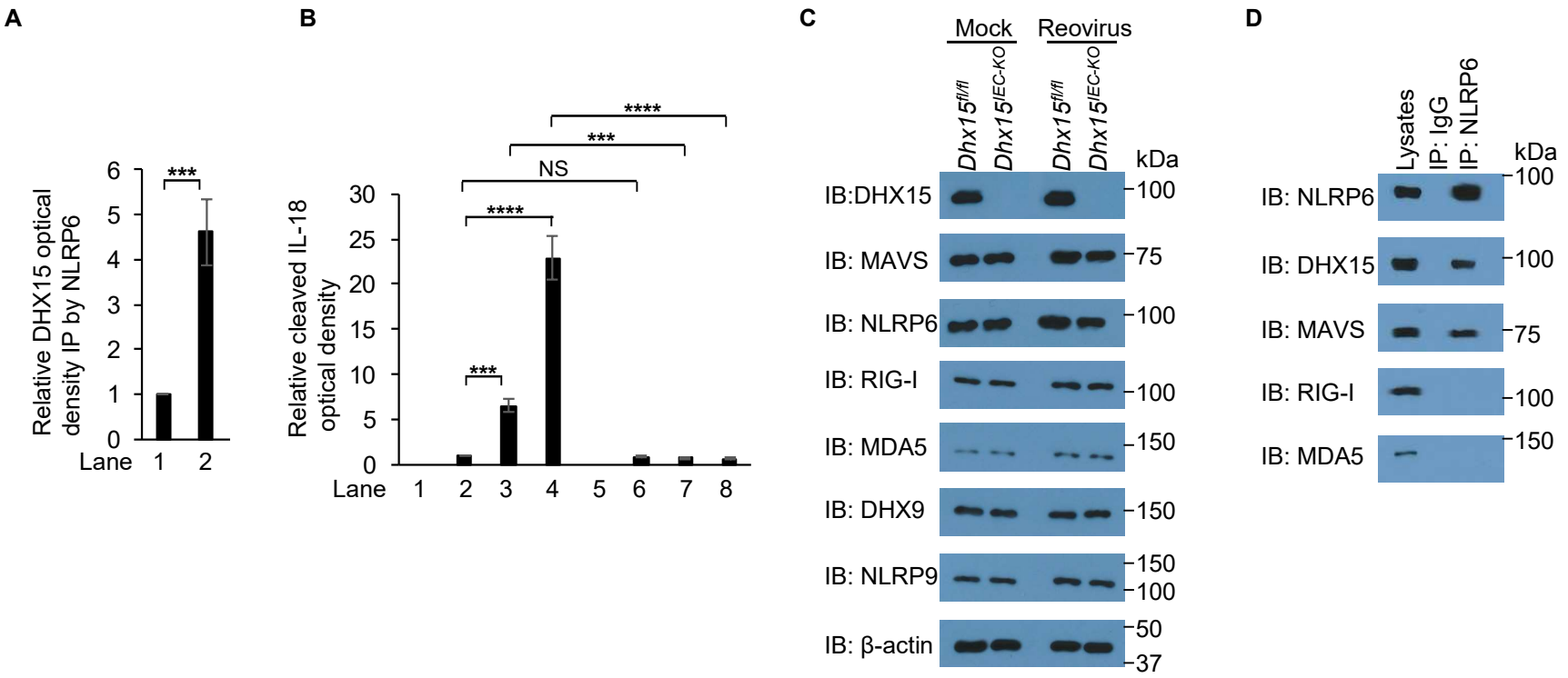

Figure S9. DHX15 recruits MAVS and NLRP6 to form signaling complex in mouse IECs after reovirus infection. Related to Figure 6.

(**A**) Quantification of immunoblot bands of DHX15 immunoprecipitated (IP) by NLRP6 in top panel of Fig. 6A expressed as relative to lane 1 using the densitometric analysis by ImageJ software; n=3 blots.

(**B**) Quantification of immunoblot bands of cleaved IL-18 in fifth panel of Fig. 6E expressed as relative to lane 2 using the densitometric analysis by ImageJ software; n=3 blots. NS, not significant, ***P<0.001, ****P<0.0001 (unpaired t test).

(**C**) Immunoblot (IB) analysis of the expression of RNA sensors including DHX15, DHX9, RIG-I and MDA5 and adaptors including MAVS, NLRP6 and NLRP9 in mouse primary IECs from wild-type *Dhx15*$^{fl/fl}$ and *Dhx15*$^{IEC\text{-}KO}$ mice without or with reovirus infection at MOI of 1 for 1 hour.

(**D**) Immunoblot analysis of endogenous proteins of NLRP6, DHX15, MAVS, RIG-I and MDA5 precipitated with anti-NLRP6 or control IgG from whole-cell lysates of mouse IECs from wild-type *Dhx15*$^{fl/fl}$ mice infected with reovirus at MOI of 10 for 6 hours. The position of protein markers (shown in kDa) is indicated on the right.

Table S1. Primers for qRT-PCR and genotype PCR used in this study. Related to STAR Methods.

Gene	Sequence
qRT-PCR	
Human *Gapdh*	F: 5'- GGAGCGAGATCCCTCCAAAAT -3'
	R: 5'- GGCTGTTGTCATACTTCTCATGG -3'
Mouse *Ifnb*	F: 5'- CCCTATGGAGATGACGGAGA -3'
	R: 5'- TCCCACGTCAATCTTTCCTC -3'
Mouse *Ifnl2/3*	F: 5'- AGTGGAAGCAAAGGATTG -3'
	R: 5'- GAGATGAGGTGGGAACTG -3'
Mouse *Il18*	F: 5'- GCCTCAAACCTTCCAAATCA -3'
	R: 5'- TGGATCCATTTCCTCAAAGG -3'
Mouse *Gapdh*	F: 5'- AGGTCGGTGTGAACGGATTTG -3'
	R: 5'- TGTAGACCATGTAGTTGAGGTCA -3'
Mouse *Hprt*	F: 5'- CACAGGACTAGAACACCTGC -3'
	R: 5'- GCTGGTGAAAAGGACCTCT -3'
Mouse *E-cadherin*	F: 5'- CACCTGGAGAGAGGCCATGT -3'
	R: 5'- TGGGAAACATGAGCAGCTCT-3'
Mouse *Claudin-2*	F: 5'- TATGTTGGTGCCAGCATTGT-3'
	R: 5'- TCATGCCCACCACAGAGATA-3'
Mouse *Occludin*	F: 5'- CCTCCAATGGCAAAGTGAAT-3'
	R: 5'- CTCCCCACCTGTCGTGTAGT-3'
Mouse *ZO-1*	F: 5'- CCACCTCTGTCCAGCTCTTC -3'
	R: 5'- CACCGGAGTGATGGTTTTCT -3'
Mouse *β-actin*	F: 5'- CGTGAAAAGATGACCCAGATCA -3'
	R: 5'- CACAGCCTGGATGGCTACGT -3'
Rotavirus NSP5	F: 5'- TTCTGCTTCAAACGAYCCACTC -3'
	R: 5'- GAGAAATCYACTTGRTCGCA -3'
Reovirus S4	F: 5'- GGAACATTGTGAGAGCAGCA -3'
	R: 5'- GCAAGCTAGTGGAGGCAGTC -3'
HSV-1 VP16	F: 5'- TCGGCGTGGAAGAAACGAGAGA -3'
	R: 5'- CGAACGCACCCAAATCGACA -3'
Dhx15 genotype PCR	
P1	5'-CACCCAAGTATCAGTATTCTCACG -3'
P2	5'-GCAATAATGTAACACAGCTAACAGC -3'
P3	5'-GATTGGTTTCTCTAATTGCTAGCC -3'
P4	5'-CACTGTGTGAGTTCAAGAATCACC -3'
Villin-Cre genotype PCR	
Common primer 16775	5'-GCCTTCTCCTCTAGGCTCGT -3'
WT primer 16776	5'-TATAGGGCAGAGCTGGAGGA -3'
Mutant primer oIMR9074	5'-AGGCAAATTTTGGTGTACGG -3'